Characterization of Cu(II) Bipyridine Complexes in Halogen Atom Transfer Reactions by Electron Spin Resonance

Bernhard Knuehl,[†] Tomislav Pintauer,[‡] Atsushi Kajiwara,[‡,§] Hanns Fischer,*[,†] and Krzysztof Matyjaszewski*[,‡]

Physikalisch-Chemisches Institut der Universitaet Zuerich, Winterthurerstrasse 190, CH 8057 Zuerich; Department of Chemistry, Carnegie Mellon University, 4400 Fifth Avenue, Pittsburgh, Pennsylvania 15213; and Nara University of Education, Takabatake-cho, Nara 630-8528, Japan

Received May 28, 2003; Revised Manuscript Received August 14, 2003

ABSTRACT: Electron spin resonance was used to investigate structural features of Cu^{II} complexes with dNbpy (4,4′-di(5-nonyl)-2,2′-bipyridine) and d*n*Nbpy (4,4′-di-*n*-nonyl-2,2′-bipyridine) ligands in methyl isobutyrate (MIB) and toluene. With 1 or 2 equiv of either dNbpy or d*n*Nbpy ligands, $Cu^{II}Br_2$ forms predominantly the neutral complexes Cu^{II}(dNbpy)Br_2 and Cu^{II}(d*n*Nbpy)Br_2, respectively. Bromine atom transfer between $[Cu^{I}(dnNbpy)_2]^+[Cu^{I}Br_2]^-$ and ethyl 2-bromoisobutyrate (EBriB) in MIB does not yield Cu^{II}(d*n*Nbpy)Br_2. Instead, it leads to the complex $[Cu^{II}(dnNbpy)_2Br]^+[Cu^{I}Br_2]^-$. The latter species is also formed in an equilibration reaction of Cu^{II}(d*n*Nbpy)Br_2 with $[Cu^{I}(dnNbpy)_2]^+[Cu^{I}Br_2]^-$ ($K \geq 100$ $M^{-1/2}$, 23 °C, MIB).

Introduction and Background

The synthesis of macromolecules with well-defined compositions, architectures, and functionalities represents an ongoing effort in the field of polymer chemistry. Over the past few years, atom transfer radical polymerization (ATRP) has emerged as a very powerful and robust technique to meet these goals.[1−5] The basic working mechanism of ATRP (Scheme 1) involves a reversible switching between two oxidation states of a transition-metal complex.[3,6,7] Typically, copper(I) halide is used in conjunction with a nitrogen-based complexing ligand.[8,9]

Homolytic cleavage of the alkyl halide bond (R−X) by the $Cu^{I}X/L_n$ complex generates an alkyl radical R• and the corresponding $Cu^{II}X_2/L_n$ complex. The radical R• can propagate with a rate constant k_p by adding to the double bond of a vinyl monomer, terminate by either coupling or disproportionation (k_t), or be reversibly deactivated by the Cu^{II} complex (k_{deact}). The contribution of radical termination is reduced as a result of the persistent radical effect,[10,11] and the equilibrium is strongly shifted toward the dormant species ($k_{act} \ll k_{deact}$). Consequently, polymers with predictable molecular weights, narrow molecular weight distributions, and high functionalities can be synthesized.[12]

Structural and mechanistic studies are crucial to further understand this mechanism and are inherently part of the future developments in ATRP. The important factors that need to be considered in the structural aspects of ATRP include the structures of the catalysts in solution and their solvent and temperature dependence,[13−20] the role of complexing ligand and its influence on the catalyst properties (e.g., redox potential),[21] the participation of the catalyst in side reactions other than atom transfer,[22−27] and the characterization of other active intermediates (e.g., radicals).[28] Mechanistic studies, on the other hand, should aim at determining the rate constants for elementary reactions occurring in the ATRP such as activation, deactivation, and initiation[29−35] and more importantly correlate them with reaction parameters such as catalyst, alkyl halide and monomer structure, temperature, and solvent.[36−38] Such studies can lead to a development of optimal catalysts for specific monomers and reaction conditions and generally improve the overall catalytic process. In this paper, we report the results of an electron spin resonance (ESR) study of Cu^{II} complexes with dNbpy (4,4′-di(5-nonyl)-2,2′-bipyridine) and d*n*Nbpy (4,4′-di-*n*-nonyl-2,2′-bipyridine) ligands (Scheme 2) in methyl isobutyrate (MIB) and toluene. Furthermore, the structural features of a mixed Cu^{I}/Cu^{II}/d*n*Nbpy complex generated during bromine atom transfer between $[Cu^{I}(dnNbpy)_2]^+[Cu^{I}Br_2]^-$ and ethyl 2-bromoisobutyrate (EBriB) as well as by the reaction of $[Cu^{I}(dnNbpy)_2]^+[Cu^{I}Br_2]^-$ with Cu^{II}(d*n*Nbpy)Br_2 are discussed.

Scheme 1. Proposed Mechanism for ATRP

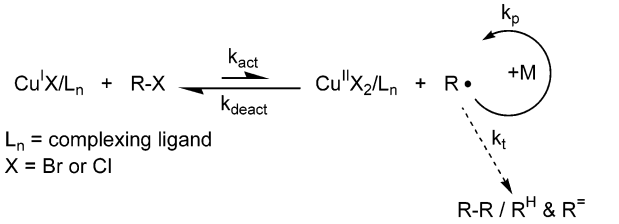

Scheme 2. 4,4′-Di(5-nonyl)-2,2′-bipyridine (dNbpy) and 4,4′-Di-*n*-nonyl-2,2′-bipyridine (d*n*Nbpy) Ligands Used in Copper-Based ATRP

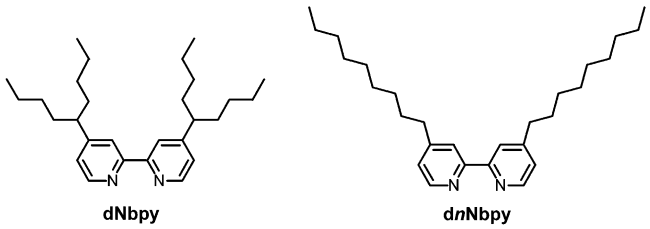

[†] Physikalisch-Chemisches Institut der Universitaet Zuerich.
[‡] Carnegie Mellon University.
[§] Nara University of Education.
* Corresponding authors. E-mail: hfischer@pci.unizh.ch; km3b@andrew.cmu.edu.

10.1021/ma0347161 CCC: $25.00
Published on Web 10/07/2003

Experimental Section

All chemicals were purchased in the purest available forms from Fluka or Aldrich. TEMPO (2,2,6,6-tetramethylpiperidine-*N*-oxyl) was purified by sublimation at room temperature under reduced pressure. 4,4′-Di(5-nonyl)-2,2′-bipyridine (dNbpy) was synthesized according to a literature procedures.[39] The solvents, methyl isobutyrate (MIB) and toluene, were dried by refluxing over CaH_2 before distillation. All chemicals were stored and all solutions were prepared in a glovebox (MBraun MB 150B-G) under nitrogen with an oxygen content of <10 ppm.

ESR spectra were recorded with a Bruker EMX spectrometer equipped with the variable temperature unit ER 4111 VT or with a Bruker ESP-300 X-band ESR spectrometer. Cu^{II} concentrations were determined from double integrals by calibration with solutions of TEMPO in the same solvent taking into account different spectrometer settings. To obtain coupling constants, simulations of ESR spectra were performed with the Public EPR Software Tools WinSim of the National Institute of Environmental Health (NIEHS). *g*-factors were estimated from the magnetic field at the spectral center and the microwave frequency.

Reproducible results were only obtained if oxygen and water were carefully excluded. ESR sample tubes were cleaned by rinsing with concentrated H_2SO_4, a cleaning fluid (Neodisher LM3), acetone, and distilled water, and these and all other glassware were dried under vacuum at 150 °C and 200 mbar before use and kept in the glovebox. Sample tubes with Cu^{II} solutions were closed with a glass stopcock only, whereas those containing Cu^{I} complexes were freed from gases by several freeze−pump−thaw cycles on a vacuum line and sealed off under vacuum.

Results and Discussion

Complexes of $Cu^{II}Cl_2$ and $Cu^{II}Br_2$ with dnNbpy and dNbpy Ligands. Unsubstituted 2,2′-bipyridine was the first ligand used in copper-mediated ATRP.[8] Alkyl substituents in the 4- and 4′-positions of the bipyridine ring, such as in the dNbpy and d*n*Nbpy ligands (Scheme 2), further improved the solubility of the catalyst in nonpolar media, which resulted in higher conversions with very low polydispersities.[40]

The complexes used in this study were prepared by adding water-free copper(II) halides and the complexing ligands d*n*Nbpy or dNbpy to MIB, which is a solvent that resembles methyl methacrylate. Complexation was accelerated by sonification. Without added ligands, the halides do not dissolve, and according to ESR, the maximum concentration of dissolved complexes is about 1 mM. Solutions prepared with 0.5 mM concentrations of $Cu^{II}Cl_2$ and 1 and 2 equiv of the d*n*Nbpy ligand were light blue. They showed identical ESR structures and intensities (cf. Supporting Information, Figure 1). This indicates 1:1 stoichiometry between d*n*Nbpy and Cu^{II}. The same was observed for $Cu^{II}Br_2$ solutions containing 1 or 2 equiv of d*n*Npy or dNbpy ligand. They had a red-violet color. For equal concentrations of $Cu^{II}Cl_2$ and $Cu^{II}Br_2$ and the same ligand concentration, the total ESR intensities (double integrals) were identical, as expected. This is consistent with earlier spectroscopic studies.[16]

Figure 1 shows the ESR spectrum of a solution containing 0.5 mM $Cu^{II}Cl_2$ and 0.5 mM d*n*Nbpy in MIB at 23 °C. It consists of a 1:1:1:1 quartet caused by hyperfine coupling to one copper nucleus ($I = {}^3/_2$). The widths of the individual lines differ markedly and decrease to the high field side of the spectrum. A reasonable simulation (overlay in Figure 1) leads to $a(Cu^{II}) = 72$ G (7.2 mT) and line widths of 43, 35, 30, and 27 G, with uncertainties of a few gauss. The *g*-factor was estimated as $g = 2.12(0.01)$. The simulation shows some minor deficiencies. These may be due to different couplings of the two magnetic copper isotopes (^{63}Cu: 69.2% atomic couplings $a = 213.9$ mT; ^{65}Cu: 30.8%, $a = 228.9$ mT),[41] unresolved Cl hyperfine couplings, and/or different line shapes of the individual lines which were not taken into account.

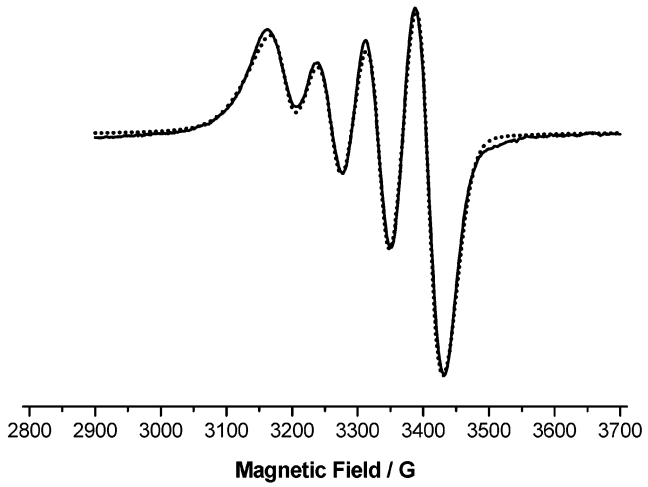

Figure 1. ESR spectrum of 0.5 mM $Cu^{II}Cl_2$ and 0.5 mM d*n*Nbpy in methyl isobutyrate (MIB) at 23 °C (solid line) and simulated spectrum (dotted line).

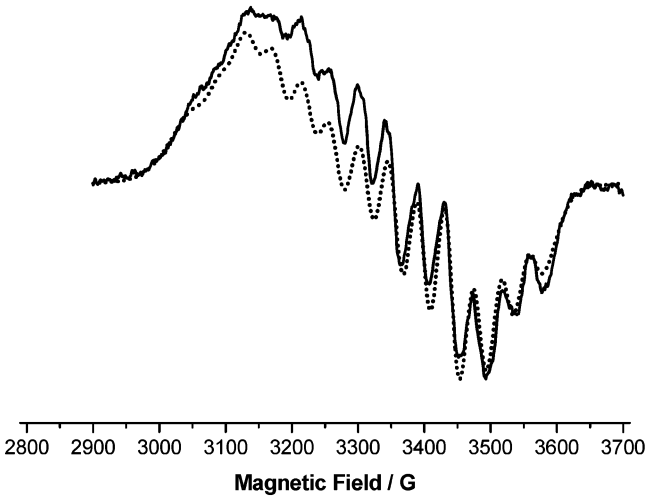

Figure 2. ESR spectrum of 0.5 mM $CuBr_2$ and 0.5 mM d*n*Nbpy in MIB at 23 °C (solid line) and simulated spectrum (dotted line).

Spectra like that shown in Figure 1 are common for Cu(II)−amine complexes in liquid solution.[42] In comparison with the literature, the coupling constants, *g*-factors, and line widths are comparable.[42] They are known, however, to depend markedly on the ligand, the counterion, the solvent, and the temperature.

Figure 2 shows the spectrum of a solution of 0.5 mM $Cu^{II}Br_2$ and 0.5 mM d*n*Nbpy in MIB at 23 °C. A similar spectrum was also observed for the dNbpy ligand. The overlaying simulation describes the number and the positions of the lines correctly and is based on one coupling copper nucleus ($a = 86$ G) and two equally coupling bromine nuclei ($a = 41.5$ G). The line widths again decrease somewhat toward the high field side of the spectrum as 35, 30, 33, and 23 G, and the line shapes also differ throughout the spectrum. The *g*-factor is $g = 2.11(0.01)$, and the estimated errors are as indicated above for the $Cu^{II}Cl_2$/d*n*Nbpy complex. The bromine hyperfine structure of $Cu^{II}Br_2$/d*n*Nbpy com-

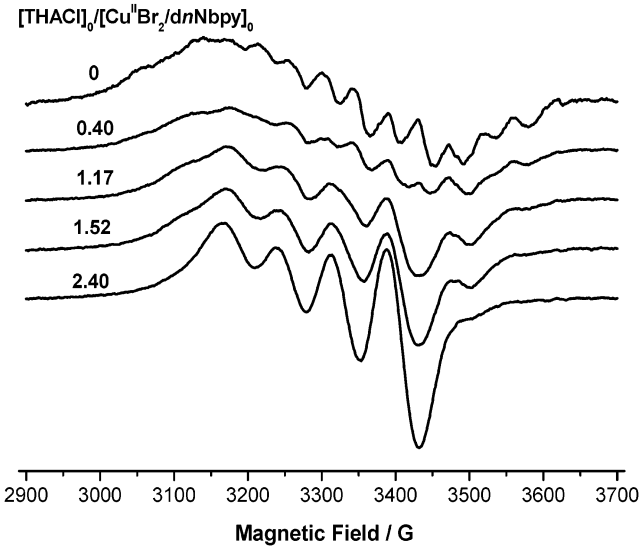

Figure 3. ESR spectra of 0.5 mM $CuBr_2$ and 0.5 mM d*n*Nbpy in MIB at 23 °C containing different amounts of tetra-*n*-heptylammonium chloride (THACl).

plexes seems to be unknown so far. It is not unlikely, in view of the large atomic couplings of the bromine isotopes which are much larger than those of the Cu or Cl isotopes (^{79}Br: 50.7%, atomic couplings $a = 1144.3$ mT; ^{81}Br: 49.3%, $a = 1233.5$ mT; ^{35}Cl: 75.8%, $a = 204.2$ mT; and ^{37}Cl: 30.8%, $a = 170.0$ mT).[41] Deficiencies of the simulation are likely due to the reasons outlined above and in addition to the inequivalency of the Br isotopes and possibly different line widths of the Br hyperfine lines within the Cu lines which were not considered. In view of the large line widths, couplings to ligand H or N atoms should not be resolved because they have much smaller atomic couplings.[41]

The spectrum obtained in MIB solvent was similar to that observed in toluene solutions. For this solvent, the spectrum did not change when the temperature was increased to 80 °C, but lost resolution and broadened somewhat upon cooling below 0 °C. Probably the latter feature is related to the well-known fluxionality of Cu^{II} complexes.[41,43,44]

The above results suggest 1:1 stoichiometry between $Cu^{II}X_2$ (X = Cl or Br) and d*n*Nbpy or dNbpy ligands in nonpolar media such as MIB and toluene. This is further supported by the following experimental observations. When one adds increasing amounts of tetra *n*-heptylammonium chloride (THACl) to a solution of 0.5 mM $Cu^{II}Br_2$ and 0.5 mM d*n*Nbpy in MIB, the spectrum of Figure 2 is increasingly substituted by that of Figure 1. The exchange is complete for 2.4 equiv of THACl (Figure 3). Very likely, Cl^- is more strongly bound to Cu^{2+} than Br^- so that the 2.4 equiv needed for complete exchange indicates two halide ions both for Cu^{II}(d*n*Nbpy)Cl_2 and Cu^{II}(d*n*Nbpy)Br_2. Second, addition of increasing amounts of solid $Cu^{II}Br_2$ to 0.5 mM d*n*Nbpy in MIB causes a linear increase of the ESR intensity up to a 1:1 ratio of $Cu^{II}Br_2$:d*n*Nbpy ligand. (cf. Supporting Information, Figure 2) An excess $Cu^{II}Br_2$ does not dissolve. The intensity of the signal was calibrated with a standard TEMPO solution of 0.5 mM and behaved according to expectation.

The results described above are fully consistent with our previous investigation of the $Cu^{II}Br_2$/dNbpy system in a nonpolar medium, including monomers that are typically used in the ATRP.[13−16,20] In the solid state, Cu^{II}(dNbpy)Br_2 has a near square planar geometry and belongs to the C_{2v} point group, indicating the equivalence of N and Br atoms.[16] The Cu^{II} center is coordinated by the two nitrogen atoms of a single dNbpy ligand (Cu^{II}−N = 2.011(7) and 2.022(7) Å)) and two bromine atoms (Cu^{II}−Br = 2.3621(14) and 2.3567(13) Å). Similar structural features have also been observed for Cu^{II}(bpy)Br_2[45] and Cu^{II}(bpy)Cl_2[46] complexes. The stoichiometry between $Cu^{II}Br_2$ and dNbpy as well as average Cu^{II}−N and Cu^{II}−Br bond distances do not vary in nonpolar media, as shown by UV−vis spectroscopic[16] and extended X-ray absorption fine structure (EXAFS) studies.[15] Contrary to nonpolar media, in polar solvents such as CH_3CN, DMF, and MeOH, $Cu^{II}Br_2$ and dNbpy predominantly form the ionic 2:1 complex, $[Cu^{II}(dNbpy)_2Br]^+[Br]^-$.[16]

Cu^{II}/dnNbpy Complexes in the Presence of Cu^{I}/dnNbpy Complexes and in ATRP. During ATRP, Cu^{I} and Cu^{II} species exist simultaneously in the reaction solution (Scheme 1). To mimic the catalytic system in the ATRP more closely, EPR studies were conducted on Cu^{II}/d*n*Nbpy complexes that were generated during atom transfer between Cu^{I}Br/d*n*Nbpy and alkyl halide. Additionally, the species formed by the reaction of Cu^{I}Br/d*n*Nbpy with Cu^{II}(d*n*Nbpy)Br_2 were investigated.

Cu^{I}Br is insoluble in MIB but dissolves upon addition of d*n*Nbpy ligand. Completely oxygen-free solutions of Cu^{I}Br and d*n*Nbpy in MIB are dark brown and do not exhibit an ESR signal. On admission of oxygen, even only in traces and inadvertently, Cu^{I}Br/d*n*Nbpy solutions develop a blue color and show a 1:1:1:1 quartet with a(Cu) ≈ 77 G and g ≈ 2.15 and line widths decreasing to the high field side. The spectrum is similar to but less resolved than that of Figure 1. The quartet is accompanied by a weaker narrow signal with five or seven evenly spaced lines with about 15 G separation at $g \approx 2.00$ (higher field) which must be due to a rather persistent organic radical. It may be a nitroxide radical formed from the ligand but could not be identified (cf. Supporting Information, Figure 3). Cu^{I}/amine complexes react with oxygen and form oxo and peroxo complexes which are stable at low temperature.[47] At higher temperatures some of the reported reactions such as the coupling of secondary amines or of phenols point to radical chemistry.[48,49] It has also been reported that ATRP can be induced by oxygen in initiator-free systems,[50,51] and the above observation may be relevant to this. The following experiments refer to oxygen-free solutions as evidenced by their color and absence or only very small contributions of the quartet of the oxidated species to the ESR spectra.

To check for the appearance of a Cu^{II} signal during a Br transfer reaction, a solution of 1 mM Cu^{I}Br, 1 mM d*n*Nbpy, and 10 mM EBriB in MIB was heated for several hours at 120 °C. Trace a in Figure 4 presents the final spectrum. It is quite different from that assigned to Cu(d*n*Nbpy)Br_2 (Figure 2), but very similar to the spectra obtained in real ATRP systems.[52,53] The final conversion of Cu^{I} to Cu^{II} was about 40%. An ESR signal at 3260 G could be due to a small contribution of the oxidation product.

From a variety of spectroscopic and kinetic results,[16,37] we have proposed the final product of atom transfer to be $[Cu^{II}(dnNbpy)_2Br]^+[Cu^{I}Br_2]^-$ in less polar media such as that used here. To further confirm the stoichiometry and structure of the ATRP generated $[Cu^{II}(dnNbpy)_2Br]^+[Cu^{I}Br_2]^-$ complex, ESR studies of solutions

Scheme 3. Proposed Equilibrium for the Reaction of $[Cu^{I}(d(n)Nbpy)_2]^{+}[Cu^{I}Br_2]^{-}$ with $Cu^{II}(d(n)Nbpy)Br_2$

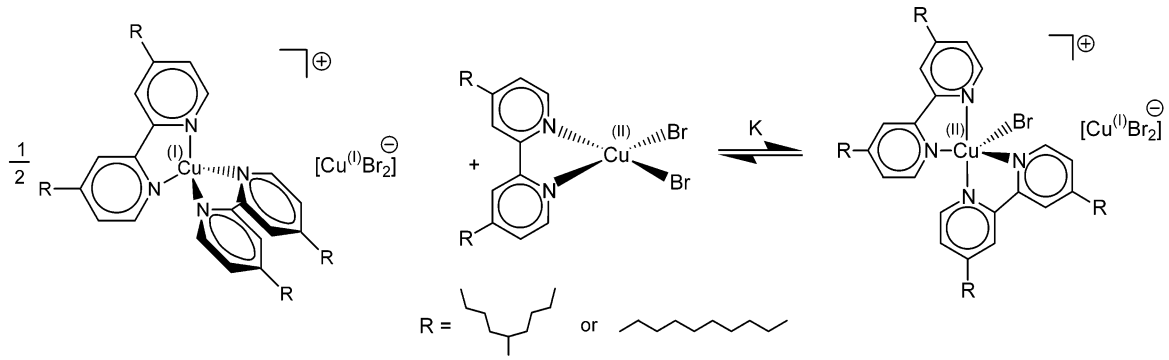

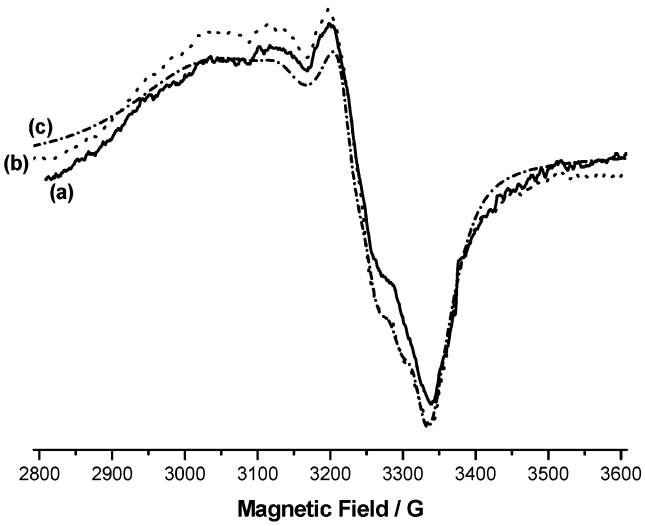

Figure 4. ESR spectra in MIB at 23 °C of solutions containing (a) 1 mM $Cu^{I}Br$, 1 mM d*n*Nbpy, and 10 mM ethyl 2-bromoisobutyrate (after heating for several hours at 120 °C), (b) $Cu^{I}Br$, $Cu^{II}Br_2$, and d*n*Nbpy in molar ratio 1:1:2, and (c) simulation of spectrum b.

containing $Cu^{I}Br$, $Cu^{II}Br_2$, and d*n*Nbpy in the molar ratio 1:1:2 were conducted.

As indicated in Figure 4, the spectrum of a solution containing $Cu^{I}Br$, $Cu^{II}Br_2$, and d*n*Nbpy in the ratio 1:1:2 in MIB at 23 °C (trace b) is nearly identical to that of trace a. The simulation (Figure 4, trace c) reproduces the features fairly well with couplings to one $I = {}^3/_2$ nucleus with $a = 68$ G and a second $I = {}^3/_2$ nucleus with $a = 33$ G and $g = 2.16(0.01)$. Comparison with the values given above for $Cu^{II}(dnNbpy)Br_2$ suggests that the larger coupling belongs to Cu and the smaller to Br. There is no resolvable coupling to a second Cu or a second Br. This agrees with the structure $[Cu^{II}(dnNbpy)_2Br]^{+}[Cu^{I}Br_2]^{-}$.

Similar results were also obtained in the case of dNbpy ligand in toluene (Figure 5). The ESR spectrum of $Cu^{II}Br_2$/2dNbpy complex in toluene at 25 °C (Figure 5, trace a) resembles that found in MIB (Figure 2) and is different than the spectrum of $Cu^{I}Br/Cu^{II}Br_2$/2dNbpy mixture at the same temperature (Figure 5, trace c). This is consistent with the findings for the d*n*Nbpy ligand and the presence of $Cu^{II}(dNbpy)Br_2$ and $[Cu^{II}(dNbpy)_2Br]^{+}[Cu^{I}Br_2]^{-}$ complexes. However, at −223 °C the two systems yield nearly identical spectra (Figure 5, traces b and d), which indicates similar structures of the complexes at lower temperatures. Our earlier investigation of the $Cu^{II}Br_2$/dNbpy system in nonpolar media such as toluene indicated that the neutral

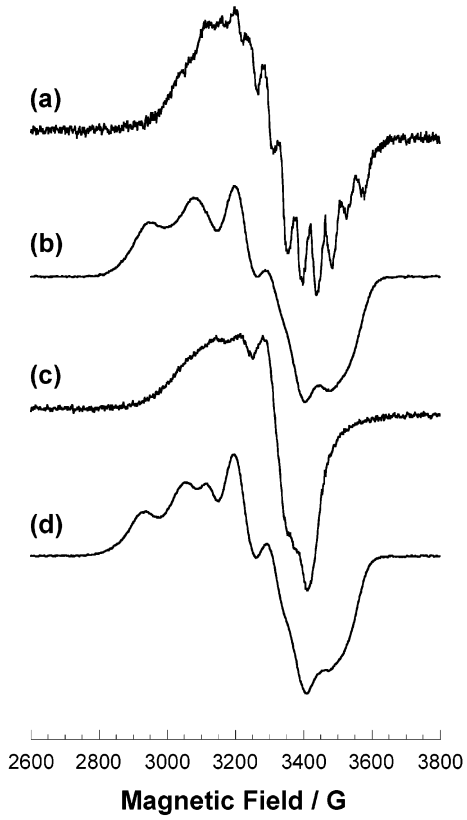

Figure 5. ESR spectra of $Cu^{II}Br_2$/2dNbpy (25 °C (a) and −223 °C (b)) and $Cu^{I}Br/Cu^{II}Br_2$/2dNbpy (25 °C (c) and −223 °C (d)) in toluene.

$Cu^{II}(dNbpy)Br_2$ complex in the presence of dNbpy ligand undergoes Br substitution to form the ionic $[Cu^{II}(dNbpy)_2Br]^{+}[Br]^{-}$ complex.[16] The enthalpy ($\Delta H° = -39.2$ kJ mol^{-1}) and entropy ($\Delta S° = -110$ J K^{-1} mol^{-1}) for this equilibrium reaction in toluene[16] suggest that at −223 °C the $Cu^{II}Br_2$ complex with 2 equiv of dNbpy ligand predominantly forms the ionic $[Cu^{II}(dNbpy)_2Br]^{+}[Br]^{-}$ complex, contrary to room temperature at which $Cu^{II}(dNbpy)Br_2$ is strongly preferred. The similarity of the traces b and d in Figure 5 is therefore due to the presence of $[Cu^{II}(dNbpy)_2Br]^{+}$ cations and further supports that the $Cu^{I}Br/Cu^{II}Br_2$/2dNbpy mixture results in the formation of the $[Cu^{II}(dNbpy)_2Br]^{+}[Cu^{I}Br_2]^{-}$ complex.

The above findings show that the $[Cu^{I}(d(n)Nbpy)_2]^{+}$-$[Cu^{I}Br_2]^{-}$ complex reacts with $Cu^{II}(d(n)Nbpy)Br_2$ to generate $[Cu^{II}(d(n)Nbpy)_2Br]^{+}[Cu^{I}Br_2]^{-}$, as presented in Scheme 3. To investigate this reaction further, solutions of 1 mM $Cu^{I}Br$/d*n*Nbpy and 1 mM $Cu^{II}Br_2$/d*n*Nbpy were

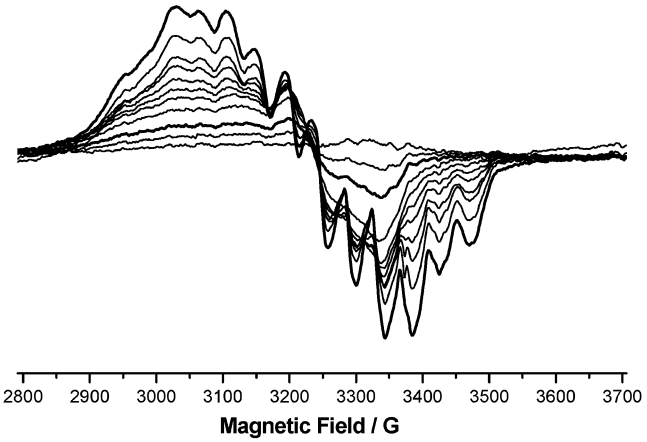

Figure 6. ESR spectra of mixtures of 1 mM solutions of $Cu^{II}Br_2$/d*n*Nbpy and $Cu^{I}Br$/d*n*Nbpy in MIB at 23 °C with total [Cu] = 1 mM. Larger intensities correspond to larger fractions of Cu^{II} (cf. Figure 7 for the exact fractions of Cu^{II}).

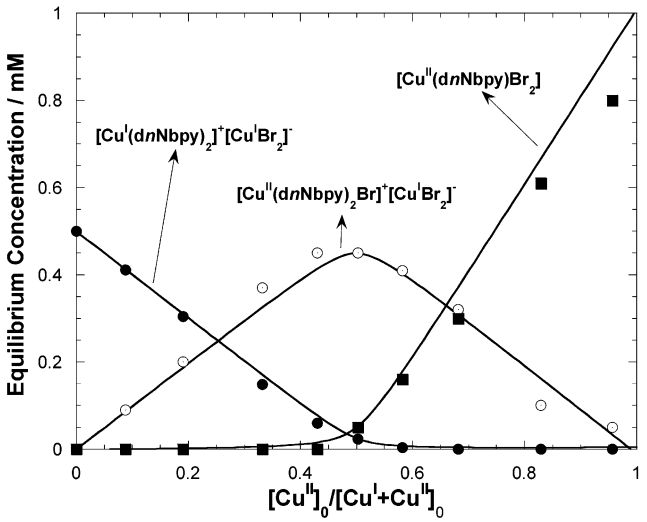

Figure 7. Equilibrium concentrations of Cu^{I} and Cu^{II} species as a function of the fraction of Cu^{II} for $Cu^{I}Br$/d*n*Nbpy and $Cu^{II}Br_2$/d*n*Nbpy mixtures in Figure 5 with total [Cu] = 1 mM. Theoretical lines were calculated assuming $K \geq 100$ $M^{-1/2}$.

prepared and mixed in various ratios so that the total [Cu] and ligand concentrations were constant at 1 mM. ESR spectra are shown in Figure 6 (increase in total intensity corresponds to larger fractions of Cu^{II}). Figure 6 also indicates that for small concentrations of $Cu^{II}Br_2$/d*n*Nbpy the spectrum resembles that of Figure 4, whereas for large ones, the spectrum of Figure 2 is reobtained. Simulating the spectra as superpositions of the spectra given in Figures 2 and 4 lead to the equilibrium concentrations of Cu^{II}(d*n*Nbpy)Br_2 and $[Cu^{II}(dn\text{Nbpy})_2Br]^+[Cu^{I}Br_2]^-$. A plot of these and $[Cu^{I}(dn\text{Nbpy})_2]^+[Cu^{I}Br_2]^-$ against the fraction of added Cu^{II} complex ($[Cu^{II}]_0/[Cu^{I}+Cu^{II}]_0$) is shown in Figure 7. The calculation took into account the stoichiometry of the $[Cu^{I}(dn\text{Nbpy})_2]^+[Cu^{I}Br_2]^-$ complex (i.e., 1 mL of $Cu^{I}Br$ and 1 mL of d*n*Nbpy forms 0.5 mM $[Cu^{I}(dn\text{Nbpy})_2]^+[Cu^{I}Br_2]^-$). The data are accommodated by theoretical lines calculated from the law of mass action with a rather large equilibrium constant $K \geq 100$ $M^{-1/2}$. Some deviations may be due to imprecise mixing ratios. The equilibrium constant ($K \geq 100$ $M^{-1/2}$) for the reaction presented in Scheme 3 indicates that the addition of $Cu^{II}Br_2$/d*n*Nbpy depletes the total concentration of $Cu^{I}Br$/d*n*Nbpy complex and must be therefore taken into account when evaluating the performance of $Cu^{I}Br$/d*n*Nbpy-catalyzed ATRP systems that contain the external $Cu^{II}Br_2$/d*n*Nbpy complex. Furthermore, it also indicates that the complex Cu^{II}(d*n*Nbpy)Br_2 cannot be present in solutions containing a large excess of $[Cu^{I}(dn\text{Nbpy})_2]^+[Cu^{I}Br_2]^-$, which is typical for ATRP. The same findings also hold for the dNbpy ligand.

The number of ligand molecules in $[Cu^{II}(dn\text{Nbpy})_2Br]^+[Cu^{I}Br_2]^-$ was further confirmed by titration experiments. Solid $Cu^{I}Br$ and $Cu^{II}Br_2$ were added to MIB in amounts that would correspond to 1 mM each if the compounds were completely dissolved. Then, d*n*Nbpy was added in different amounts, and ESR spectra of the solutions were taken. The maximum intensity was reached for a ligand concentration slightly above 2 mM (cf. Supporting Information, Figure 4). For ligand concentrations below 1 mM, only Cu^{II}(d*n*Nbpy)Br_2 was observed, whereas for larger ones $[Cu^{II}(dn\text{Nbpy})_2Br]^+[Cu^{I}Br_2]^-$ dominated. This is understandable because the formation of Cu^{II}(d*n*Nbpy)Br_2 requires one and that of $[Cu^{II}(dn\text{Nbpy})_2Br]^+[Cu^{I}Br_2]^-$ two d*n*Nbpy molecules per Cu^{II}. Overall, the signal intensity saturation at close to 2 mM d*n*Nbpy concentration confirms the stoichiometry of the $[Cu^{II}(dn\text{Nbpy})_2Br]^+[Cu^{I}Br_2]^-$ complex.

Addition of EBriB to solutions of $[Cu^{II}(dn\text{Nbpy})_2Br]^+[Cu^{I}Br_2]^-$ brought no change of the spectra. The same was observed in the presence of oxidant CF_3SO_3Ag (cf. Supporting Information, Figure 5). These results indicate that $[Cu^{II}(dn\text{Nbpy})_2Br]^+[Cu^{I}Br_2]^-$ is fairly resistant against further oxidation or, in other words, that $[Cu^{I}Br_2]^-$ anions do not participate in Br atom transfer. The inactivity of $[Cu^{I}Br_2]^-$ anions in ATRP has been observed previously.[17,40]

These results suggest that some earlier reported values of k_{act} with bpy type ligands in nonpolar media may need to be corrected, since concentration of the true activator $Cu^{I}(bpy)_2^+$ is smaller than that of the initially added $Cu^{I}Br$. Therefore, the concentration of the $Cu^{I}Br_2^-$ anion, which is a counterion to both $Cu^{I}(bpy)_2^+$ and $Cu^{III}(bpy)_2Br^+$ cations, should be subtracted from $[Cu^{I}Br]_0$. Thus, $[Cu^{I}(bpy)_2^+] = ([Cu^{I}Br]_0 - [Cu^{II}Br_2]_0)/2$.

Subject to further investigation is the ESR study of other Cu^{II} complexes, such as those of PMDETA (*N*,*N*′,*N*″,*N*″-pentamethyldiethylenetriamine) and Me_6TREN (tris[2-(dimethylamino)ethyl]amine) ligands, which are also active in ATRP.

Acknowledgment. The financial support from the CMU CRP Consortium, the NSF grant (CHE-0096601), and the Swiss National Foundation for Scientific Research is greatly appreciated.

Supporting Information Available: ESR spectra recorded under various conditions and examples of superimposition and simulation. This material is available free of charge via the Internet at http://pubs.acs.org.

References and Notes

(1) *Controlled Radical Polymerization*; Matyjaszewski, K., Ed.; ACS Symposium Series Vol. 685; American Chemical Society: Washington, DC, 1998.
(2) *Controlled/Living Radical Polymerization: Progress in ATRP, NMP and RAFT*; Matyjaszewski, K.; Ed.; ACS Symposium Series Vol. 768; American Chemical Society: Washington, DC, 2000.
(3) Matyjaszewski, K.; Xia, J. *Chem. Rev.* **2001**, *101*, 2921−2990.
(4) Kamigaito, M.; Ando, T.; Sawamoto, M. *Chem. Rev.* **2001**, *101*, 3689−3745.

(5) *Handbook of Radical Polymerization*; Matyjaszewski, K.; Davis, T. P., Eds.; John Wiley & Sons: Hoboken, 2002.
(6) Matyjaszewski, K. *Chem.—Eur. J.* **1999**, *5*, 3095−3102.
(7) Patten, T. E.; Matyjaszewski, K. *Acc. Chem. Res.* **1999**, *32*, 895−903.
(8) Wang, J.-S.; Matyjaszewski, K. *J. Am. Chem. Soc.* **1995**, *117*, 5614−5615.
(9) Patten, T. E.; Xia, J.; Abernathy, T.; Matyjaszewski, K. *Science* **1996**, *272*, 866−868.
(10) Fischer, H. *Chem. Rev.* **2001**, *101*, 3581−3610.
(11) Fischer, H. *J. Polym. Sci., Part A: Polym. Chem.* **1999**, *37*, 1885−1901.
(12) Coessens, V.; Pintauer, T.; Matyjaszewski, K. *Prog. Polym. Sci.* **2001**, *26*, 337−377.
(13) Kickelbick, G.; Pintauer, T.; Matyjaszewski, K. *New J. Chem.* **2002**, *26*, 462−468.
(14) Kickelbick, G.; Reinohl, U.; Ertel, T. S.; Weber, A.; Bertagnolli, H.; Matyjaszewski, K. *Inorg. Chem.* **2001**, *40*, 6−8.
(15) Pintauer, T.; Reinohl, U.; Feth, M.; Bertagnolli, H.; Matyjaszewski, K. *Eur. J. Inorg. Chem.* **2003**, 2082−2094.
(16) Pintauer, T.; Qiu, J.; Kickelbick, G.; Matyjaszewski, K. *Inorg. Chem.* **2001**, *40*, 2818−2824.
(17) Levy, A. T.; Olmstead, M. M.; Patten, T. E. *Inorg. Chem.* **2000**, *39*, 1628−1634.
(18) Haddleton, D. M.; Duncalf, D. J.; Kukulj, D.; Crossman, M. C.; Jackson, S. G.; Bon, S. A. F.; Clark, A. J.; Shooter, A. J. *Eur. J. Inorg. Chem.* **1998**, 1799−1806.
(19) Haddleton, D. M.; Clark, A. J.; Duncalf, D. J.; Heming, A. M.; Kukulj, D.; Shooter, A. J. *J. Chem. Soc., Dalton Trans.* **1998**, 381−385.
(20) Pintauer, T.; Jasieczek, C. B.; Matyjaszewski, K. *J. Mass Spectrom.* **2000**, *35*, 1295−1299.
(21) Qiu, J.; Matyjaszewski, K.; Thouin, L.; Amatore, C. *Macromol. Chem. Phys.* **2000**, *201*, 1625−1631.
(22) Pintauer, T.; Tsarevsky, N. V.; Kickelbick, G.; Matyjaszewski, K. *Polym. Prepr. (Am. Chem. Soc., Div. Polym. Chem.)* **2002**, *43* (2), 221−222.
(23) Pintauer, T.; McKenzie, B.; Matyjaszewski, K. *Polym. Prepr. (Am. Chem. Soc., Div. Polym. Chem.)* **2002**, 217−218.
(24) Haddleton, D. M.; Perrier, S.; Bon, S. A. F. *Macromolecules* **2000**, *33*, 8246−8251.
(25) Schon, F.; Hartenstein, M.; Muller, A. H. E. *Macromolecules* **2001**, *34*, 5394−5397.
(26) Bednarek, M.; Biedron, T.; Kubisa, P. *Macromol. Chem. Phys.* **2000**, *201*, 58−66.
(27) Matyjaszewski, K.; Davis, K. A.; Patten, T. E.; Wei, M. *Tetrahedron* **1997**, *53*, 15321−15329.
(28) Yu, Q.; Zeng, F.; Zhu, S. *Macromolecules* **2001**, *34*, 1612−1618.
(29) Pintauer, T.; Zhou, P.; Matyjaszewski, K. *J. Am. Chem. Soc.* **2002**, *124*, 8196−8197.
(30) Matyjaszewski, K.; Paik, H.-j.; Zhou, P.; Diamanti, S. J. *Macromolecules* **2001**, *34*, 5125−5131.
(31) Goto, A.; Fukuda, T. *Macromol. Rapid Commun.* **1999**, *20*, 633−636.
(32) Ohno, K.; Goto, A.; Fukuda, T.; Xia, J.; Matyjaszewski, K. *Macromolecules* **1998**, *31*, 2699−2701.
(33) Matyjaszewski, K. *J. Macromol. Sci., Pure Appl. Chem.* **1997**, *A34*, 1785−1801.
(34) Auke, S.; Klumperman, B.; Van der Linde, R. *Macromolecules* **2002**, *35*, 4785−4790.
(35) Chambard, G.; Klumperman, B.; German, A. L. *Macromolecules* **2002**, *35*, 3420−3425.
(36) Nanda, A. K.; Matyjaszewski, K. *Macromolecules* **2003**, *36*, 1487−1493.
(37) Nanda, A. K.; Matyjaszewski, K. *Macromolecules* **2003**, *36*, 599−604.
(38) Matyjaszewski, K.; Gobelt, B.; Paik, H.-j.; Horwitz, C. P. *Macromolecules* **2001**, *34*, 430−440.
(39) Hadda, T. B.; Bozec, H. L. *Polyhedron* **1988**, *7*, 575−577.
(40) Matyjaszewski, K.; Patten, T. E.; Xia, J. *J. Am. Chem. Soc.* **1997**, *119*, 674−680.
(41) Weil, J. A.; Bolton, J. R.; Wertz, J. E. *Electron Paramagnetic Resonance*; Wiley: New York, 1994.
(42) Chiang, T.-C. *J. Chem. Phys.* **1968**, *48*, 1814−1818.
(43) Hathaway, B.; Billing, D. E. *Coord. Chem. Rev.* **1970**, *5*, 143−207.
(44) Hathaway, B.; Duggan, M.; Murph, A.; Mullane, J.; Power, C.; Walsh, A.; Walsh, B. *Coord. Chem. Rev.* **1981**, *36*, 267−324.
(45) Hammond, R. P.; Cavaluzzi, M.; Haushalter, R. C.; Zubieta, J. A. *Inorg. Chem.* **1999**, *38*, 1288−1292.
(46) Garland, M. T.; Grandjean, D.; Spodine, E.; Atria, A. M.; Manzur, J. *Acta Crystallogr., Sect. C: Cryst. Struct. Commun.* **1988**, *44*, 1209−1212.
(47) Caulton, K. G.; Davies, G.; Holt, E. M. *Polyhedron* **1990**, *19*, 2319−2351.
(48) Kajimoto, T.; Takahashi, H.; Tsujii, J. *Bull. Chem. Soc. Jpn.* **1982**, *55*, 3673−3674.
(49) Kitajima, N.; Moro-oka, Y. *Chem. Rev.* **1994**, *94*, 737−757.
(50) Ersin, A. A.; Yagci, M. B.; Mathias, L. J. *Macromolecules* **2000**, *33*, 7700−7706.
(51) Nanda, A. K.; Hong, S. C.; Matyjaszewski, K. *Macromol. Chem. Phys.* **2003**, *204*, 1151−1159.
(52) Kajiwara, A.; Matyjaszewski, K.; Kamachi, M. *Macromolecules* **1998**, *31*, 5695−5701.
(53) Kajiwara, A.; Matyjaszewski, K. *Macromol. Rapid Commun.* **1998**, *19*, 319−321.

MA0347161